Observational Study

Medicine

OPEN

Investigating the efficacy of immune checkpoint inhibitors in clear cell renal cell carcinoma based on methylation cross talk scoring

Qinglong Du, MD[a,b], Qiyuan Wang, BA[a,b], Chen Yang, BA[a,b], Yiping Wang, BA[a,b], Huiyang Yuan, MD[a], Bing Zhang, MD[c], Hong Ji, MD[d], Shuai Fu, MD[e], Chunlei Xue, MD[f,*]

Abstract

Methylation processes in different molecular contexts (DNA, RNA, and histones) are controlled by different regulatory factors and serve as critical determinants in cancer development. However, the mechanistic links between these epigenetic modifications during malignant transformation, metastasis, disease relapse, and therapeutic resistance remain incompletely understood. In this research, we investigated the transcriptional and genetic alterations of regulators associated with 3 major types of methylation modifications in clear cell renal cell carcinoma. Utilizing ChIP/MeRIP-seq and 450K methylation array data, we identified genes regulated by multiple methylation modifications and constructed a scoring model to quantify the methylation patterns for each patient. Our findings indicate that patients with a low score may be more likely to respond to immunotherapy, whereas patients with a high score may be more sensitive to targeted therapy, such as RITA, Pazopanib, Irlotinib, SU-11274, BRD-K16762525, and FCCP. In conclusion, the score model can serve as a valuable biomarker to guide clinical selection of immunotherapy and targeted drugs and help to improve personalized clear cell renal cell carcinoma treatment.

Abbreviations: ccRCC = clear cell renal cell carcinoma, CMap = Connectivity Map, ICB = immune checkpoint blockade, KIRC = kidney renal clear cell carcinoma, LASSO = least absolute shrinkage and selection operator, MMCscore = methylation-modification crosstalk score, TCGA = The Cancer Genome Atlas, TME = tumor microenvironment.

Keywords: crosstalk of methylation modification, gene-targeted therapies, immunotherapy, personalized therapy, renal cancer

1. Introduction

As one of the major challenges of global health issues, the incidence and mortality rate of kidney cancer remain high, among which clear cell renal cell carcinoma (ccRCC) is one of the most important subtypes.[1] Surgical removal of tumor lesions is currently the main treatment method, but about 30% to 40% of patients still experience postoperative recurrence and metastasis, leading to poor postoperative outcomes.[2] While new targeted therapies and immune checkpoint blockade (ICB) have shown success in improving the clinical prognosis of metastatic renal cell carcinoma, the majority of metastatic cases still ultimately result in patient mortality.[3] Therefore, the identification of new prognostic biomarkers and therapeutic targets is crucial for improving the survival rate of patients with ccRCC.

Epigenetics is an important branch of genetics that reversibly produces new phenotypes without changing the DNA sequence.[4] This modification process plays a vital role in the occurrence, development, and prognosis of cancer. Among them, DNA methylation, RNA methylation, and histone modification are the 3 most common and important aspects.[5,6] The re These modifications are precisely regulated by specific enzymes such as methyltransferases, demethylases, and binding proteins, forming an intricate regulatory network and providing a wide range of crosstalk sites for modifications in different dimensions.[7,8] For example, the coordinated generation of DNA methylation (5-methylcytosine [5mC]), RNA modification (N6-methyladenosine [m6A]), and histone methylation can reshape the tumor microenvironment (TME), alter cellular phenotypes, and promote cell growth and evasion of immune surveillance.[9–14] Therefore, an in-depth study of the interactions

The authors have no funding and conflicts of interest to disclose.

The datasets generated during and/or analyzed during the current study are available from the corresponding author on reasonable request.

Supplemental Digital Content is available for this article.

[a] Department of Urology, Qilu Hospital of Shandong University, Jinan, Shandong, China, [b] Cheeloo College of Medicine, Shandong University, Jinan, Shandong, China, [c] Department of Urology, Qilu Hospital of Shandong University (Qingdao), Qingdao, China, [d] Department of Pathology, Qilu Hospital of Shandong University (Qingdao), Qingdao, China,[e] Shandong Cancer Hospital and Institute, Shandong First Medical University and Shandong Academy of Medical Sciences, Jinan, People's Republic of China, [f] Department of Urology, Qilu Hospital of Shandong University Dezhou Hospital, Dezhou, China.

** Correspondence: Chunlei Xue, Department of Urology, Qilu Hospital of Shandong University Dezhou Hospital, No.1751 Xinhu Street, Decheng District, Dezhou, Shandong Province 253000, China (e-mail: xuechunlei2006@163.com).*

How to cite this article: Du Q, Wang Q, Yang C, Wang Y, Yuan H, Zhang B, Ji H, Fu S, Xue C. Investigating the efficacy of immune checkpoint inhibitors in clear cell renal cell carcinoma based on methylation cross talk scoring. Medicine 2025;104:11(e41795).

Received: 6 November 2024 / Received in final form: 18 February 2025 / Accepted: 19 February 2025

http://dx.doi.org/10.1097/MD.0000000000041795

of different methylation modifications can provide important clues for the development of new prognostic biomarkers and therapeutic targets.

ICB therapy, as an important part of cancer immunotherapy, is a major breakthrough in cancer treatment in recent years and has shown significant efficacy in many types of cancer.[15] However, due to the diverse and intricate nature of the tumor immune microenvironment, along with the ongoing genetic alterations in tumor cells, immunotherapy proves to be ineffective for the majority of patients with advanced tumors. Therefore, it is very important to search for molecular markers that can accurately predict the efficacy of ICB. However, the commonly used indicators such as PD-L1 expression, microsatellite instability, tumor tissue mutation load, tumor-infiltrating lymphocytes, and PBRM1 gene mutation cannot very accurately identify metastatic renal cell carcinoma patients who are effective against ICB. In this study, we revealed the impact of DNA, RNA, and histone methylation modifications in ccRCC on the tumor immune microenvironment of ccRCC patients through in-depth analysis of these modifications, thereby guiding the personalized application of immunotherapy. Using ChIP/MeRIP-seq and 450K methylation array data, we found that the cross talk of different dimensional methylation modifications was prevalent and identified many genes regulated by more than 1 type of methylation modification. By studying the expression of regulatory factors associated with the prognosis of ccRCC, we identified 3 different clusters. Using differentially expressed genes in different clusters, we constructed a scoring model. This model assesses whether a patient can benefit from immunotherapy or other drugs by quantifying the level of differentially expressed genes in different clusters for each patient. We found that patients with low scores are a potential target population for immunotherapy. Patients with high scores are potential targets for genome-targeted therapies, including RITA, pazopanib, irinotecan-A, SU-11274, BRD-K16762525, and FCCC. The score model is a valuable biomarker to guide clinical immunotherapy and targeted drug selection and help to improve personalized ccRCC treatment.

2. Methods

2.1. Data source and handling

The Cancer Genome Atlas (TCGA) provides somatic mutation data, RNA sequencing data, and clinical information of patients with ccRCC, specifically from the renal clear cell carcinoma (KIRC) cohort. The Xena database provides copy number variation data for patients, where "0" indicates no variation. "1" and "2" indicate amplification. "−1" and "−2" indicate deletion. The clinical information corresponding to the TCGA RNA sequencing data is shown in Table S1 (Supplemental Digital Content, http://links.lww.com/MD/O481).[16,17] We further selected 4 datasets from the Gene Expression Omnibus and ArrayExpress databases (E-MTAB-2007, E-MTAB-1980, GSE86091, and GSE138274) for validation. The raw data for ChIP-seq (GSE86091, single-end reads) and MeRIP-seq (GSE138274, paired-end reads) were quality controlled and aligned to the original publications.[18,19] IMvigor210 cohort, an anti-PD-L1 cohort, came from http://research-pub.gene.com/IMvigor210Corebiologies. Patients with ccRCC were exposed to immune checkpoint inhibitors (ICIs), ICIs combined with Bevacizumab, and Sunitinib in the IMmotion150[20,21] and IMmotion151 trials.[22,23]

2.2. Screening of methylation modification-related genes

MACS2 and exomePeak2 were used to screen the differentially methylation modified site between tumor samples and normal samples.[24,25] In general, H3K4 trimethylation (H3K4me3) modifications enriched at promoters can increase the expression of target genes.[9,26] At the same time, enriched at 3'Untranslated Region or Coding DNA Sequence region, m6A modifications can also upregulate the expression of target genes.[27] The high level of DNA methylation in the promoter can suppress the expression of target genes.[7] Genes that meet the following conditions were selected as methylation modification-related genes: differentially methylation-modified site ($P < .05$), differentially expressed genes between tumor samples and normal samples ($P < .05$; $|\text{LogFC}| \geq 1$), and positive correlation with a writer/reader or negative correlation with an eraser ($P < .05$; $|r| > 0.3$).

2.3. Genomic instability and stemness indices analysis

Based on known calculation methods, we calculated the scores for somatic copy number alteration, tumor mutation burden, homologous recombination deficiency, loss of heterozygosity, and aneuploidy.[28,29] Data for the stem cell index were obtained from the UCSC Xena database.

2.4. Self-organized classification of epigenetic regulatory patterns in DNA methylation

To characterize epigenetic regulation patterns, we conducted consensus clustering of tumor samples through expression profiling of 30 methylation-associated prognostic factors. Utilizing the ConsensusClusterPlus toolkit,[3] we implemented an iterative partitioning framework with the following computational safeguards: 1000 bootstrap replicates with 80% sample resampling per iteration, parameter constraints limiting maximum subtype number (maxK = 9), and partitioning around medoids algorithm with Euclidean metric for centroid-based partitioning.

2.5. Gene functional categorization and pathway enrichment assessment using gene ontology/Kyoto Encyclopedia of Genes and Genomes annotation systems

A comparative functional analysis of the intergene cluster expression variation that distinguishes molecular subgroups B and C was performed. Using the clusterProfiler R toolkit, we identified different biological processes through gene ontology (GO) and Kyoto Encyclopedia of Genes and Genomes (KEGG) pathway assessment to achieve pathway annotation. A significance threshold was established using the Benjamini-Hochberg correction (false discovery rate < 0.05).

2.6. Quantitative assessment of TME indices and immunological landscape characteristics

The TME was comprehensively analyzed using a dual analytical approach. The Estimation of STromal and Immune cells in MAlignant Tumor tissues using Expression data algorithm quantified the stromal and immune infiltration indices in ccRCC cases,[30] while the xCell computational framework provided detailed immune cell characterization. Complementary tumor immune dysfunction and exclusion prognostic features were obtained from the Harvard Medical School Immunotherapy Response Database (http://tide.dfci.harvard.edu/).

2.7. Construction of cross talk-related gene signature and score model

A 3-stage analytical protocol was implemented to develop prognostic biomarkers: preliminary screening via univariate Cox regression, feature selection through least absolute shrinkage and selection operator (LASSO) regularization (λ determined by minimum criteria), and final model refinement using multivariate Cox proportional hazards analysis. The composite risk score

was computed as Σ(Z-transformed expression values)/n, where n represents the signature gene count.

2.8. Drug sensitivity

The score of drug sensitivity was calculated by Connectivity Map (CMap, https://clue.io/cmap). Transcriptomic signatures comprising the top 150 up/downregulated biomarkers correlating with risk stratification profiles were cross-referenced against pharmacological databases. Therapeutic candidates demonstrating significant interaction potential were identified through stringent filtering (Z score > 1.8), with threshold-exceeding compounds advancing to mechanistic validation.

2.9. Statistical analysis

Nonparametric correlation assessments were conducted using Spearman rank-order method. Optimal survival cutoff values were identified through the survminer toolkit's maximally selected rank statistics. Other detailed statistical methods were described in figure legends. All computations were exclusively performed in the R statistical environment (version 4.0.1), with significance thresholds set at 0.05.

3. Results

3.1. ccRCC exhibits copy number and expression alterations of epigenetic modifiers

Our investigation incorporated 52 epigenetic mediators spanning 3 principal epigenetic regulation axes: DNA 5mC modification (n = 20), RNA m6A methylation (n = 23), and histone H3K4me3 events (n = 9). These regulatory components, systematically cataloged in Table S2 (Supplemental Digital Content, http://links.lww.com/MD/O481), were identified through comprehensive curation of established epigenetic mechanisms in current literature.[7,14,26,31,32]

Our initial analytical phase involved transcriptomic profiling of the TCGA-KIRC dataset (comprising 72 normal and 530 tumor specimens). Bioinformatic interrogation revealed 35 epigenetic regulators with statistically significant differential expression (Fig. 1A), displaying a polarized regulatory pattern: 80% (28/35) showing overexpression trends and 20% (7/35) demonstrating transcriptional suppression within tumor cohorts. These differentially expressed regulators indicated the important and complex role of epigenetic regulation in maintaining a neoplastic phenotype. We conducted a systematic interrogation of somatic mutation spectra associated with epigenetic regulation patterns in ccRCC cohorts. This genomic landscape analysis specifically quantified mutation burden variations across DNA methylation, RNA modification, and histone mark regulatory axes (Fig. 1B). Among 336 patients with available somatic mutation data in TCGA-KIRC cohort, 20 regulators were detected somatic mutations in more than 1% patients. Global mutation profiling revealed limited oncogenic potential among epigenetic regulators, with KDM5C (histone H3K4me3 demethylase) demonstrating the highest alteration frequency (5%). Mutational status analysis showed significant transcriptional suppression of KDM5C in altered versus unaltered genotypes (Fig. 1C). We further investigated copy number variation in these epigenetic regulators (Fig. 1D). Sixteen epigenetic regulators showed the higher frequency of copy number alterations (>1% patients). Especially, 13.92% of patients experienced copy number amplification of YTHDC2, and 14.09% of patients had a detected copy number deletion of RBM15B. The significant amplification and deletion led to increased expression of YTHDC2 and decreased expression of RBM15B, respectively (Fig. 1E and F). These findings reveal a pervasive and heterogeneous genome-epigenome interaction in the pathogenesis of ccRCC, which is characterized by recurrent alterations in methylation regulatory networks. Therefore, it is necessary to continue to study the dysregulation of methylation modification regulatory factors in depth.

3.2. Predictive value of multidimensional epigenetic cross talk in the methylation regulatory network

These epigenetic mediators fundamentally expand conventional genetic paradigms through multilayered regulatory mechanisms. To systematically investigate their inter-regulatory dynamics in oncogenesis, we conducted preliminary survival analysis through Cox proportional hazards modeling. Bioinformatic screening identified 57.7% (30/52) of epigenetic modifiers, demonstrating significant prognostic capacity (Fig. 2A), revealing functionally stratified survival patterns across methylation regulatory axes. Among these regulators, we observed 1774 coexpression events ($P < .05$; $|r| > 0.3$), which indicated the general interactions of different dimensional methylation modification (Fig. S1, Supplemental Digital Content, http://links.lww.com/MD/O480). In order to validate the previous findings, a further analysis was conducted on the Infinium HumanMethylation450 BeadChip (E-MTAB-2007), Chip-seq (GSE86091), and MeRIP-seq (GSE138274) data from the ArrayExpress database and Gene Expression Omnibus database. In comparison with normal tissues, a significant number of differentially expressed m6A regulators, including METTL3, YTHDC2, ALKBH5, METTL14, VTRMA, and so on, exhibited differential H3K4me3 modifications in tumor tissues within the TSS region (Fig. 2B and C; Fig. S2A and B, Supplemental Digital Content, http://links.lww.com/MD/O480). Meanwhile, some H3K4me3 and 5mC regulators, including SETD1B, UNG, TET1, MBD3, and ZBTB38, were accompanied by differential m6A modifications in tumor tissues of their exons (Fig. 2D and E; Fig. S2C and D, Supplemental Digital Content, http://links.lww.com/MD/O480). Similarly, many m6A and H3K4me3 regulators, like IGF2BP3, FTO, ALKBH5, and KDM5B, exhibited a differential degree of DNA methylation in their promoter region (Fig. 2F and G; Fig. S2E and F, Supplemental Digital Content, http://links.lww.com/MD/O480). Furthermore, rather than cross talk-related regulators, we also found more and more dysregulated genes accompanied by different dimensional methylation modifications. With the screening condition described in the method, we identified 1158 m6A-related genes, 510 5mC-related genes, and 2799 H3K4me3-related genes (Fig. 2H). Interestingly, 16 regulators, such as VEGFA, HHLA2, CLDN10, and so on, were coregulated by 3 types of methylation modifications (Fig. 2I–P; Fig. S2G–J, Supplemental Digital Content, http://links.lww.com/MD/O480). The above results further evidenced the active cross talk between different dimensional methylation modifications. The active cross talk plays a crucial role in tumorigenesis and immune infiltration, offering us a new horizon of epigenetic regulatory networks.

3.3. Clustering of modification regulators and immune microenvironment in unsupervised clustering

Different clusters were obtained by consensus clustering analysis of transcriptional profiles of 30 prognostically significant epigenetic modulators. The TCGA cohort of 530 ccRCC cases showed optimal partitioning into 3 clusters (Table S3, Supplemental Digital Content, http://links.lww.com/MD/O481). The heat map results of visual analysis revealed the expression of epigenetic regulatory factors in different clusters. Most of these regulatory factors were significantly overexpressed in cluster C and inhibited in cluster B (Fig. 3A). Kaplan–Meier survival curves demonstrated cluster-dependent prognostic stratification (Fig. 3B). Cluster B, characterized by epigenetic silencing signatures, exhibited the poorest clinical outcomes, while cluster C

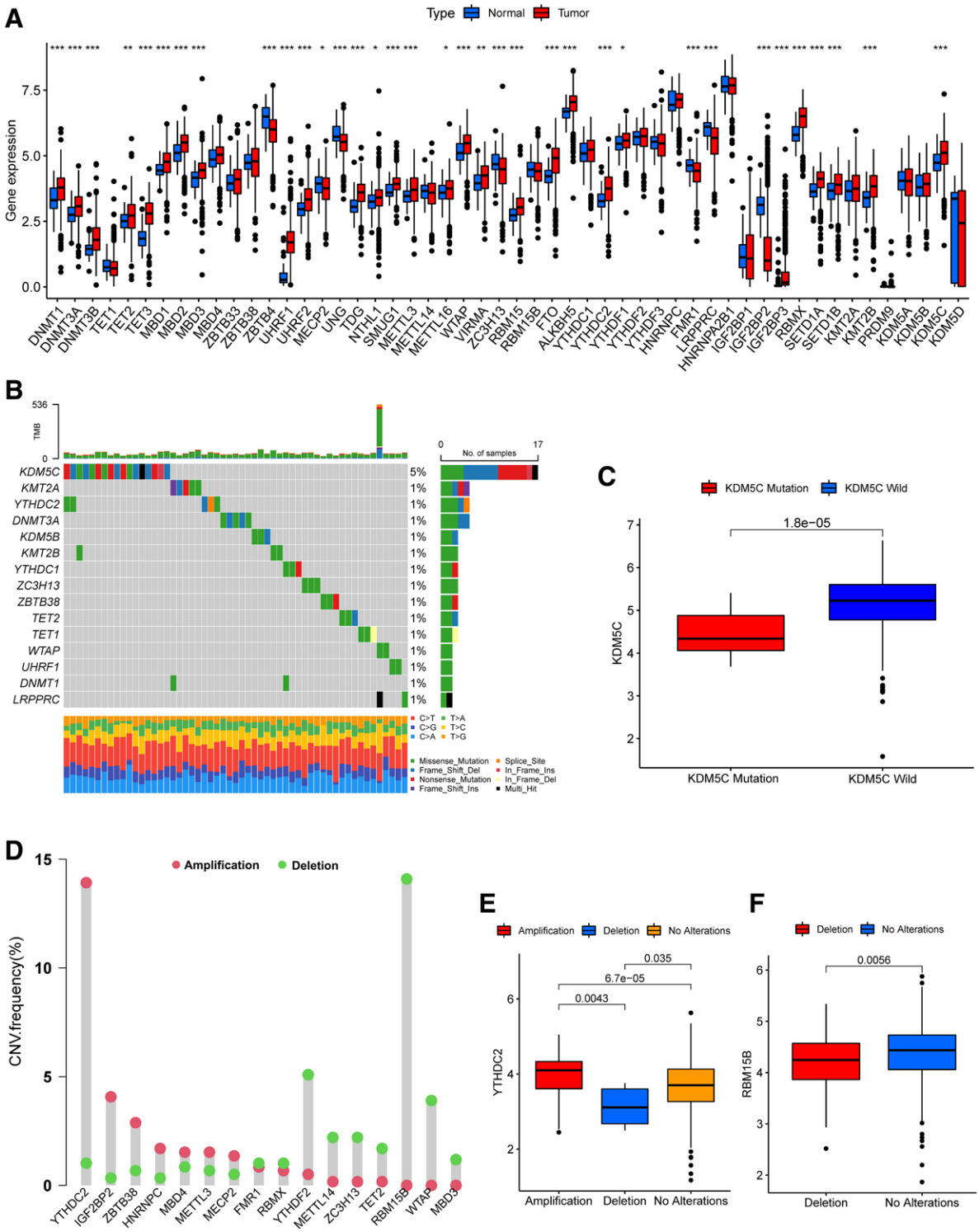

Figure 1. Clear cell renal cell carcinoma (ccRCC) exhibits copy number and expression alterations of epigenetic modifiers. (A) The distinct expression levels of methylation regulators in ccRCC tumors (n = 530) compared to normal tissues (n = 72) using data from The Cancer Genome Atlas-Kidney Renal Clear Cell Carcinoma (TCGA-KIRC) dataset using the Wilcoxon test. (B) In ccRCC patients, the mutation frequency of methylation regulators was examined. The upper panel displayed total mutation burden (TMB) values. Mutation frequencies and types were illustrated in the right panel. The lower panel depicted the proportion of conversions for each ccRCC patient. (C) The expression levels of KDM5C between wild-type and mutation-type samples using the Wilcoxon test. (D) The frequency of copy number variations (CNVs) in regulators is shown. Green dots indicate deletions, while red dots represent amplifications. (E) The expression levels of YTHDC2 across different types of copy number alterations were analyzed using the Wilcoxon test. (F) The expression levels of RBM15B were examined across different types of copy number alterations using the Wilcoxon test.

demonstrated superior survival compared to both clusters A and B. In contrast, cluster B presented higher tumor stemness, which might contribute to tumorigenesis, metastasis, and drug resistance (Fig. 3D). Then we sought to explore genomic alterations in distinct clusters. Compared with cluster C, cluster B provided a higher level of somatic copy number alteration, tumor mutation burden, homologous recombination deficiency, loss of heterozygosity, and aneuploidy (Fig. 3C). In the meantime, we

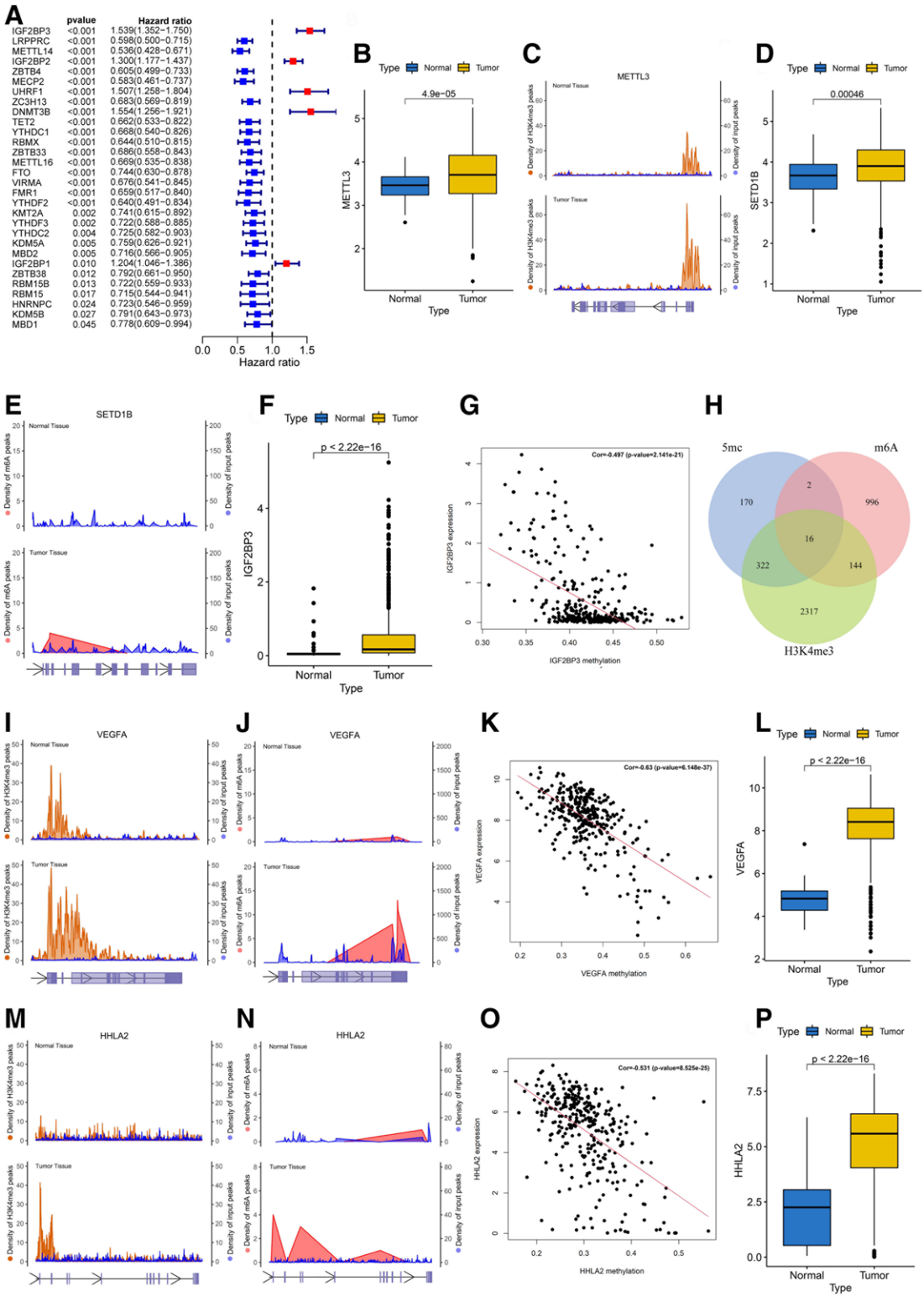

Figure 2. Predictive value of multidimensional epigenetic cross talk in the methylation regulatory network. (A) Univariate Cox regression analysis to identify regulators associated with prognosis in clear cell renal cell carcinoma (ccRCC) patients. (B and C) Differential expression (B) and density of H3k4me3 peaks (C) of METTL3 in ccRCC tumor and normal tissues. (D and E) Differential expression (D) and density of m6A peaks (E) of SETD1B in ccRCC tumor and normal tissues. (F) Differential expression of IGF2BP3 in ccRCC tumor and normal tissues. (G) Correlation analysis between the expression and DNA methylation level of IGF2BP3 in ccRCC tumor tissues using the Spearman. (H) The Venn diagram showed the intersection between different dimensional methylation modifications. (I–L) Differential expression (L), density of H3k4me3 peaks (I), and density of m6A peaks (J) of VEGFA in ccRCC tumor and normal tissues; correlation analysis (K) between the expression and DNA methylation level of VEGFA in ccRCC tumor tissues (Spearman). (M–P) Differential expression (P), density of H3k4me3 peaks (M), and density of m6A peaks (N) of HHLA2 in ccRCC tumor and normal tissues; correlation analysis (O) The relationship between HHLA2 expression and its DNA methylation levels in ccRCC tumor tissues using the Spearman.

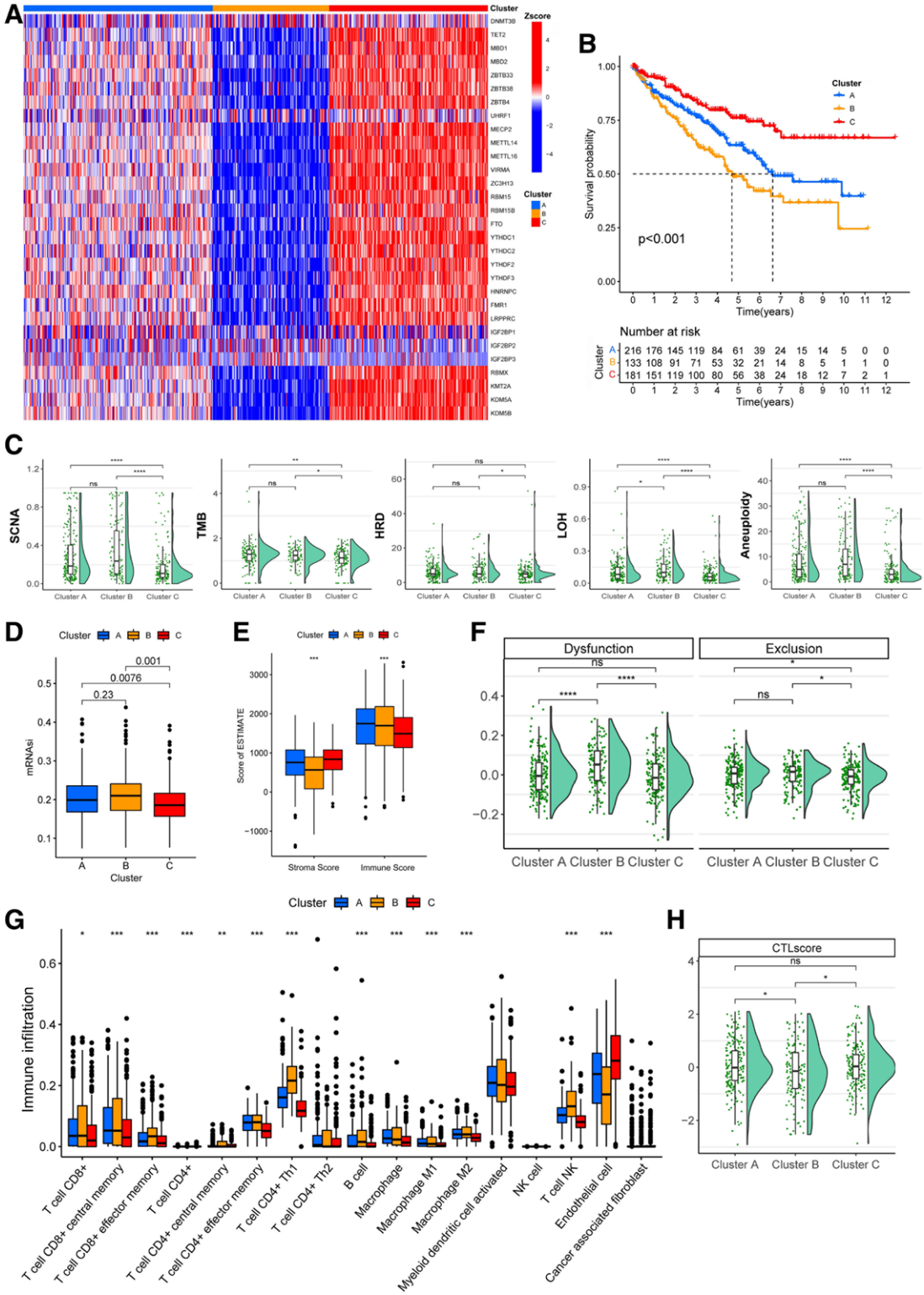

Figure 3. Clustering of modification regulators and immune microenvironment in unsupervised clustering. (A) The expression distribution of regulators in distinct clusters. (B) Overall survival of 3 distinct clusters using the log-rank test. (C) Differences of somatic copy number alteration (SCNA), total mutation burden (TMB), homologous recombination deficiency (HRD), loss of heterozygosity (LOH), and aneuploidy in distinct clusters using the Wilcoxon test. (D) Differences of stemness indices in distinct clusters. (E) Differences of Estimation of STromal and Immune cells in MAlignant Tumor tissues using Expression data score in distinct clusters. (F) Differences in dysfunction and exclusion level of $CD8^+$ T cells in distinct clusters using the Wilcoxon test. (G) The levels of immune cell infiltration across different clusters using the Wilcoxon test. (H) Differences of cytotoxic T lymphocyte (CTL) score in distinct clusters.

calculated the high and low matrix scores and immune scores in clusters B and C. The results showed that group B had a higher immune score than group C but a lower matrix score than group C (Fig. 3E). The above results suggested that cluster B, similar to hot tumor, offered a high level of antigen exposure and immune infiltration. But cluster B carried the worst prognosis. What is the reason? We used the tumor immune dysfunction and exclusion score to further explore the function

of CD8+ T cells. Even though a high level of immune infiltration was presented, cluster B was accompanied by significant dysfunction of CD8+ T cells (Fig. 3F). The calculation of the abundance of immune cells in different clusters is implemented using the R package cell. Cluster B exhibited higher CD8+ T cell infiltration, but it also infiltrated with higher immunosuppressive cells such as M2 macrophages and MDSC (Fig. 3G; Fig. S2K, Supplemental Digital Content, http://links.lww.com/MD/O480). Previous studies have shown that the cytotoxic T lymphocyte score can be calculated from the expression of the genes CD8A, CD8B, GZMA, GZMB, and PRF1.[33] Similar to the above results, the function of CD8+ T cells decreased in cluster B (Fig. 3H). The expression of some immune-activity-related markers also downregulated in cluster B, especially PRF1, TNF, CXCL10, and CXCL9 (Fig. 4A). In conclusion, all the findings suggested that it was the high level of stemness and CD8+ T cell dysfunction that led to the poor survival in cluster B.

3.4. Establishment of epigenetic methylation modification cross talk features and scoring model

In order to study the biological functions and differences between different clusters, we analyzed clusters B and C separately, and the results showed that 4738 genes were significantly differentially expressed (Table S4, Supplemental Digital Content, http://links.lww.com/MD/O481). We further studied these differentially expressed genes in depth using GO and KEGG analyses. As shown in Figure 4C to E, these genes primarily are related to the regulation of Ras protein, epithelial to mesenchymal transition, activity of helicase and telomerase, response to transforming growth factor-beta (TGF-β) and vascular endothelial growth factor receptor (VEGFR), and transcriptional regulation. The KEGG result suggested that immune response pathways were significantly enriched compared to other pathways (Fig. 4F). These differentially expressed genes were linked to PD-L1 expression and the PD-1 checkpoint pathway, T cell and B cell receptor regulation, helper T cell differentiation, and chemokine expression. We also found that many known and typical pathways were significantly enriched, including phosphatidylinositol 3-kinase-protein kinase B (PI3K-AKT) signaling, Ras signaling, Wingless/INT-1 signaling, TGF-β signaling, and Notch signaling pathway. Recent studies reported that cooccurrence and mutual exclusivity of these pathways could synergistically promote treatment resistance and immune suppression.[34,35] These findings all suggested that immune response and immunotherapy might play a substantial role in the prognosis and therapy of distinct clusters. Considering the differences between individuals, it is difficult to accurately predict an individual's situation using different clusters. Following this, the "univariate Cox - LASSO regression - multivariate Cox" workflow was used to screen the core genes to calculate the quantitative indicators (Fig. 4B). In the univariate Cox analyses, 3743 genes were correlated with overall survival. Using LASSO regression analyses to reduce dimension, 25 representative genes were retained. Finally, by multivariate Cox analyses, 9 core genes (SLC2A9, TOX3, SAA1, IFI44, DPYSL3, PDK4, ZNF521, AJAP1, and HHLA2) were identified to perform subsequent analyses. By averaging the Z-transformed expression values of the above 9 core genes, a unique score can be calculated for each patient. We define this score as the methylation modification interaction index (MMCscore). Consistent with previous findings, ccRCC patients with the lowest expression of regulators in cluster B presented the lowest MMCscore and the worst prognosis (Fig. 4G–I). This inverse relationship was clinically manifested by lower MMCscore predicting increasing clinical severity, particularly advanced histopathological progression markers, including increased tumor grading, advanced TNM staging, and metastatic spread (Fig. 4J).

3.5. Importance of MMCscore in sensitivity to ICB therapy

Immune checkpoint inhibitors targeting the PD-1/PD-L1 axis, which function by disrupting T-cell inhibitory pathways, have demonstrated improved clinical outcomes in oncology. Despite their therapeutic promise, substantial interpatient response heterogeneity persists, highlighting the critical need for standardized predictive biomarkers to optimize patient stratification and treatment protocols. To further validate the predictive effect of MMCscore in immunotherapy response, we validated it in the immunotherapy cohort (IMvigor210, anti-PD-L1 therapy). In patients with renal cancer, we found that the poor prognosis of low MMCscore group was reversed (Fig. 5A). After immunotherapy, patients with low MMCscore group presented a higher rate of objective response and better overall survival (Fig. 5B and C). Interestingly, in other urologic cancers, similar results were observed. Among bladder cancer patients, those with a better clinical prognosis tend to have a lower MMCscore (Fig. 5D–F). In urothelial cancer, although no statistically significant results were obtained, patients with a low MMCscore generally had better survival outcomes (Fig. 5G–I). These results further proved that MMCscore could not only serve as a good prognostic biomarker but also as a valuable biomarker to improve the efficacy of cancer immunotherapy.

3.6. Evaluation of external datasets for MMCscore

To verify whether the model is also applicable in other treatment datasets, we validated it in the IMmotion 150 and IMmotion 151 renal cancer immunotherapy sets (Table S5, Supplemental Digital Content, http://links.lww.com/MD/O481). Using our prognostic stratification framework developed through analytical validation, we quantified MMCscore values across the IMmotion150 and IMmotion151 study cohorts. Patients were then stratified into different risk strata (high/low) using the established prognostic threshold derived from our model. Initially, we generated a heat map to visualize the expression levels of the genes included in our model. The heat map revealed distinct expression patterns for genes such as HHLA2, SAA1, IFI44, DPYSL3, SLC2A9, TOX3, PDK4, AJAP1, and ZNF521, which exhibited varying levels between the high-risk and low-risk patients (Fig. S3A and B, Supplemental Digital Content, http://links.lww.com/MD/O480). Then, we examined the survival outcomes of patients across different groups through Kaplan–Meier analysis. We observed that patients with a high MMCscore had a lower overall survival rate compared to those with a low MMCscore. This suggests that MMCscore is an effective tool for assessing patient prognosis and serves as a dependable indicator (Fig. S3C and D, Supplemental Digital Content, http://links.lww.com/MD/O480). We subsequently created a survival status scatterplot to evaluate how well the model distinguishes between patients with different survival outcomes in the 2 treatment groups. Additionally, we generated a risk score distribution plot to assess the model's ability to differentiate between high-risk and low-risk patients across the 2 treatment cohorts (Fig. S3E–H, Supplemental Digital Content, http://links.lww.com/MD/O480). The findings from the risk curve and scatter plot reveal that patients with a high MMCscore have elevated risk factors and mortality rates compared to those with a low MMCscore. These results collectively suggest that MMCscore holds significant promise for prognostic evaluation in ccRCC patients.

3.7. Drug sensitivity of MMCscore

The above findings suggested that patients with low MMCscore were the potential target population for immunotherapy. We also wondered which drugs were preferable for patients with high MMCscore. Using CMap analysis, we found that RITA, pazopanib, irilin-a, SU-11274, BRD-K16762525, and FCCP were negatively correlated with MMScore (Fig. 6A). RITA is the MDM2 inhibitor that can target P53 and block the interaction

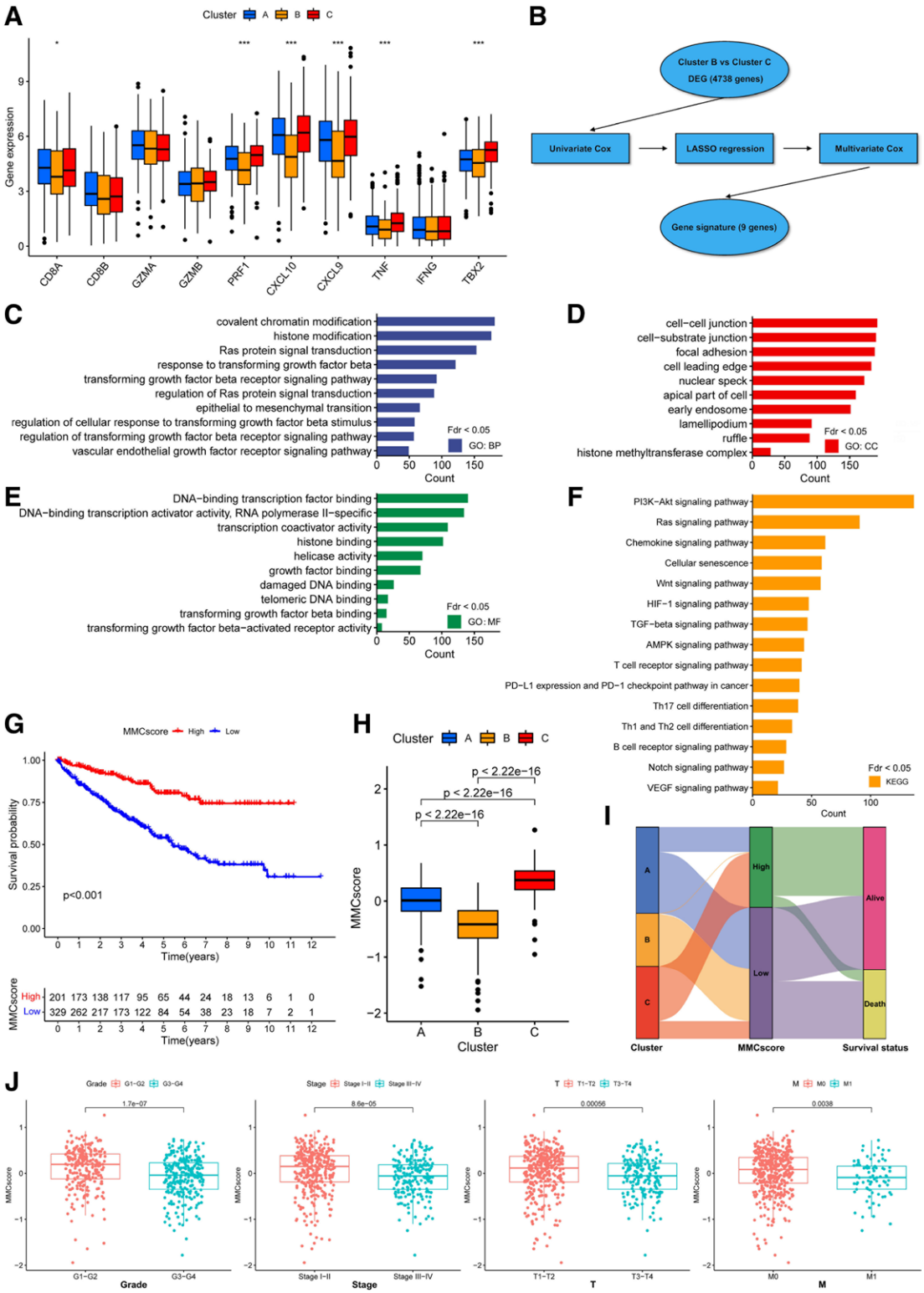

Figure 4. Establishment of epigenetic methylation modification cross talk features and scoring model. (A) Differential expression of immune-activity-related markers in distinct clusters using the Wilcoxon test. (B) The workflow of screening core genes. (C–F) Functional analysis of differentially expressed genes between clusters B and C using gene ontology (GO) and Kyoto Encyclopedia of Genes and Genomes (KEGG) pathway enrichment. (G) Survival analysis comparing low and high methylation-modification crosstalk score (MMCscore) groups via Kaplan–Meier curves using the log-rank test. (H) The distribution of MMCscore in distinct clusters. (I) Alluvial diagram of patients' distribution in groups with different cluster, MMCscore, and survival outcomes. (J) The relationships between MMCscore and clinical pathological phenotype using the Wilcoxon test.

between P53 and MDM2. Pazopanib is the VEGFR inhibitor and has been widely used in clinical treatment. The MET-targeting agent SU-11274 demonstrates specific kinase inhibition, while FCCP acts as a TGF-β pathway suppressor. In contrast, elevated expression levels of tumor-associated markers in the high-MMC cohort, including p53 signaling components (MDM2), angiogenesis regulators (VEGF/VEGFR), and TGF-β pathway elements (TGFB1/TGFBR), suggest increased activation of

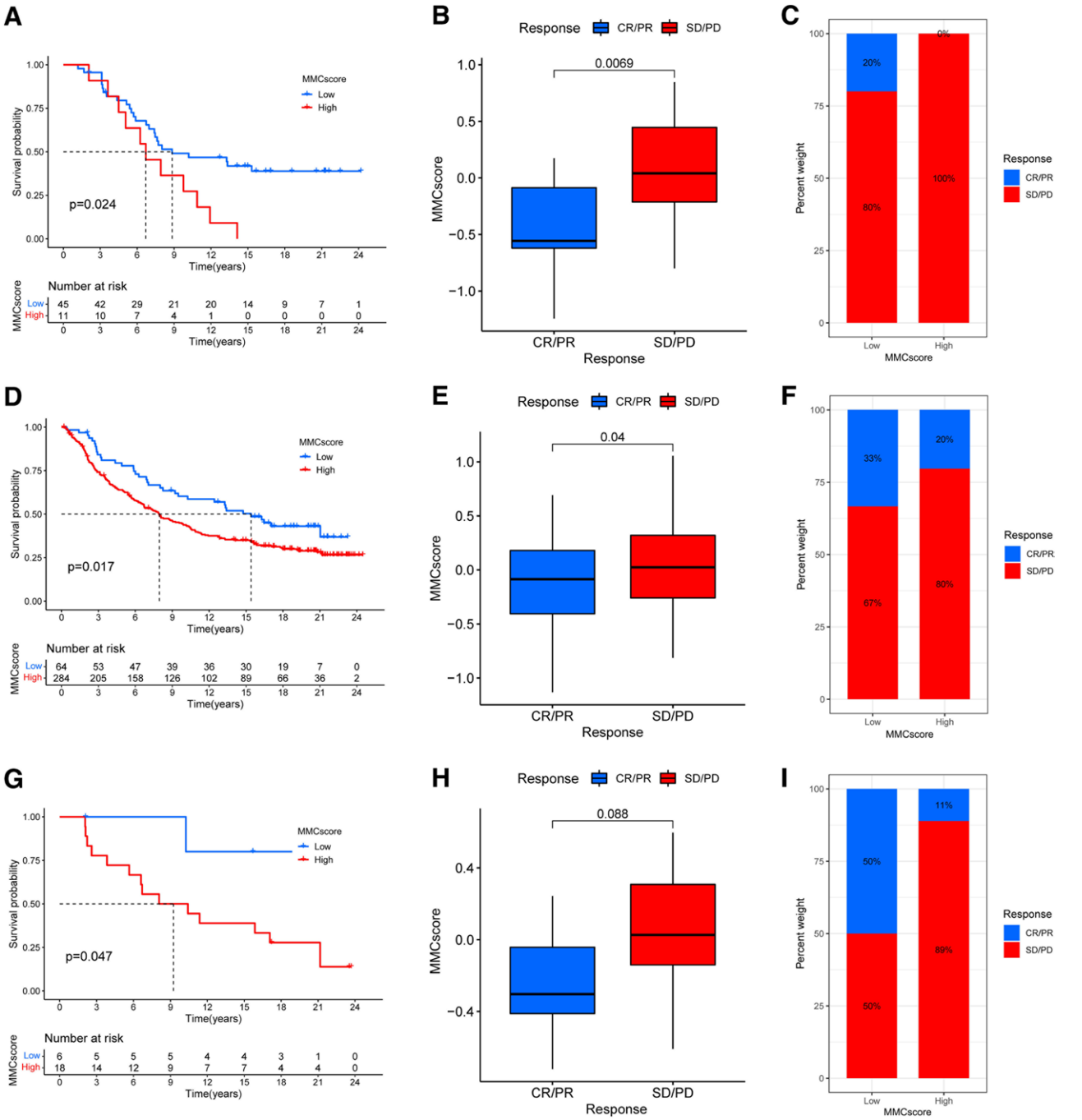

Figure 5. The importance of methylation-modification crosstalk score (MMCscore) in sensitivity to immune checkpoint blockade therapy. (A–C) The response of immunotherapy in renal cancer. (A) Overall survival of MMCscore using the log-rank test. (B and C) Different responses to immunotherapy in high and low MMCscore groups using the Wilcoxon test. (D–F) The response of immunotherapy in bladder cancer. (G–I) The response of immunotherapy in ureter cancer. CP/PR = complete response/partial response, SD/PD = stable disease/progressive disease.

oncogenic signaling (Fig. 6B). In conclusion, our results indicated that patients with low MMCscore might be suitable for immunotherapy, and RITA, pazopanib, irilin-a, SU-11274, BRD-K16762525, and FCCP might be good choices for patients with high MMCscore.

4. Discussion

The control of gene expression is a fundamental yet complex cellular mechanism. As the predominant epigenetic mechanism, DNA/RNA methylation enables phenotypic inheritance independent of changes in the genetic code.[4] Recent studies highlight that epigenetic dysregulation orchestrated by methylation modifiers critically drives oncogenic processes, including malignant transformation, modulation of the immune microenvironment, therapy resistance, and aberrant immunogenicity.[5] However, current research tends to focus narrowly on single regulatory elements or isolated components of the TME. The inter-regulatory dynamics of multilayered methylation systems and their synergistic effects on the cellular composition of the TME remain poorly characterized. Through integrated multi-omics profiling of ccRCC cohorts, our investigation comprehensively mapped both transcriptional variations and genomic instability patterns of 52 methylation-associated

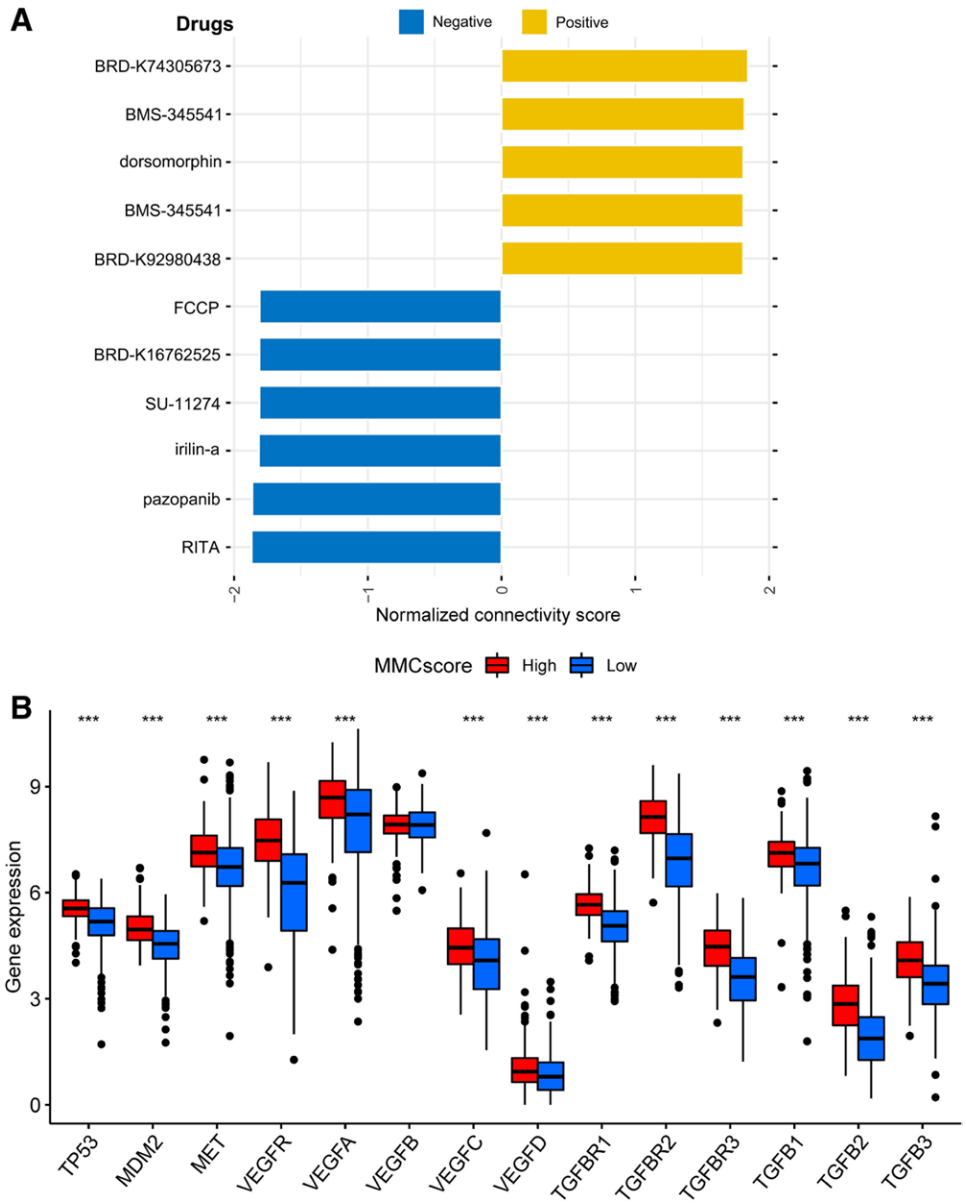

Figure 6. Drug sensitivity of methylation-modification crosstalk score (MMCscore). (A) The score of drug sensitivity was calculated by Connectivity Map. Screening criteria: normalized score > 1.8. (B) The varying expression levels of targeted genes between high and low MMCscore groups using the Wilcoxon test.

regulatory factors spanning 3 major epigenetic axes. Among these regulators, we identified 1774 cooccurrence events. Using Chip/MeRIP-seq and 450K methylation array data, we further explore the cross talk of different dimensional methylation modifications. We found that many differentially expressed regulators were regulated by other types of methylation modifications. Not only modification regulators, but many other genes were regulated by more than 1 type of methylation modification. In fact, we found that 16 regulators were simultaneously regulated by DNA, RNA, and histone methylation modification. We also found that these cross talk-related genes were correlated with tumorigenesis and immune response. These results showed that cross talk between methylation modifications of various dimensions is widespread and plays an essential role in tumor progression. Subsequently, we identified 3 distinct clusters. Cluster B presented the lowest expression of regulators and the worst prognosis, while cluster A presented the highest expression of regulators and the best prognosis. We found that cluster B exhibited higher tumor stemness than cluster C. The cancer stem cells can lead to tumorigenesis, metastasis, recurrence and therapy resistance. It may be 1 reason for the worst prognosis of Cluster B. We also found that Cluster B showed more antigen exposure and immune cell infiltration. It did not correspond to the worst prognosis. The TME of ccRCC is highly immune-infiltrated, yet immunosuppressive cell populations such as M2 macrophages and MDSCs dominate in aggressive subtypes.[36] Emerging evidence highlights that methylation modifications directly modulate immune cell function and inflammatory responses. For example, DNA hypomethylation in tumor cells can upregulate pro-angiogenic factors like VEGFA, while RNA m6A modifications regulate chemokine secretion to recruit immunosuppressive cells.[37,38] Our observation of reduced cytotoxic T cell activity in Cluster B (low MMCscore) aligns with studies showing that metabolic stress and epigenetic silencing impair T cell effector functions.[39] Furthermore, the enrichment of TGF-β and PD-1 pathways in our model underscores the dual role of methylation cross talk in shaping both immune evasion and metabolic adaptation, as recently demonstrated in ccRCC cohorts.[40] It led to the significant dysfunction of $CD8^+$ T cells

and lower cytotoxic killing ability. These results explained the reason that a high level of immune infiltration was accompanied by a poor prognosis. Comprehensively, cluster B was similar to a hot tumor (inflamed), while cluster C was similar to a cold tumor (noninflamed). For this reason, we offered a conjecture that cluster B was more suitable for immunotherapy than cluster C.

Next, we identified differentially expressed genes by comparing cluster B with cluster C. The results of GO and KEGG pathway enrichment analysis showed that the differentially expressed genes play a significant role in immune regulation mechanisms, including influencing PD-1/PD-L1 checkpoint activation, lymphocyte receptor signaling (T/B cells), the Th cell differentiation cascade, and chemokine-mediated inflammatory responses. There is also a significant enrichment in core oncogenic pathways such as PI3K-AKT/Ras signaling, the Wnt/β-catenin axis, TGF-β-Smad transduction, and Notch-mediated cell fate decisions. Recent studies have established that ccRCC is fundamentally a metabolic disease, with hallmark features including glycolytic flux partitioning, impaired mitochondrial oxidative phosphorylation, and dysregulated lipid metabolism.[41] Notably, metabolic reprogramming in ccRCC is tightly linked to epigenetic modifications. For instance, methylation cross talk has been shown to regulate cancer stem cell properties and metabolic plasticity, further driving tumor aggressiveness and therapy resistance.[42] Findings of enriched pathways such as PI3K-AKT and TGF-β signaling align with these observations, as these pathways are known to intersect with metabolic and epigenetic axes to sustain tumor progression.[43] It suggested that there was a significant difference in immune response and tumorigenesis between Cluster B and Cluster C. Given the varying characteristics among patients, it is crucial to quantify methylation modification patterns on an individual basis. Through the workflow of "univariate Cox - LASSO regression - multivariate Cox," we constructed a cross talk-related signature including 9 core genes and obtained a score (MMCscore) for each patient. The results showed that patients with a low MMCscore had a poorer prognosis and lower overall survival.

Although ICB therapy provides an effective treatment for cancer patients, its efficacy varies significantly among different patients, and it is even ineffective for some patients. In the immunotherapy cohort, we further verified the predictive value of MMCscore. Surprisingly, the rate of objective response to immunotherapy improved significantly. After immunotherapy, the worst overall survival of low MMCscore patients was reversed. At the same time, the same results were also observed in other urologic cancers. We also try to identify the suitable drugs for high MMCscore patients. Using CMap analysis, RITA, pazopanib, irilin-a, SU-11274, BRD-K16762525, and FCCP were identified as effective targeted drugs. MMCscore can serve as a meaningful biomarker to guide clinical immunotherapy and targeted drug selection. Compared with other methods, our score model combined multidimensional regulators to perform systematic analyses for the first time and is more applicable in urologic malignancies. Moreover, the signature of our model is only based on a 9-gene panel. It is more convenient and efficient to apply in clinical situations. In addition to these findings, the results of our current study require further validation in a more widely used immunotherapy population. Furthermore, the intricate interactions between methylation modifications across different dimensions warrant additional experiments for deeper exploration.

Overall, we conducted a complicated analysis of the interactions between methylation modifications across various dimensions. We quantified the patterns of methylation modifications into an individualized score called MMCscore. This model can be utilized to assess tumor pathology and malignancy levels. In addition, it helps clinicians to distinguish which patients are more suitable for immunotherapy or targeted therapy so as to provide personalized cancer treatment and better help patients achieve a good prognosis outcome.

While our study provides a robust bioinformatics framework to explore methylation cross talk, it is important to note that the MMCscore model requires validation through wet-lab experiments and prospective clinical cohorts. Future studies should include in vitro and in vivo validation using ccRCC cell lines, patient-derived organoids, or clinical specimens to confirm the functional roles of the identified regulators (e.g., HHLA2 and SAA1) and their cross talk mechanisms. Additionally, integrating multi-omics data (e.g., metabolomics and single-cell sequencing) could further elucidate the metabolic-immune-epigenetic axis in ccRCC progression and therapy resistance.

Author contributions

Data curation: Qinglong Du.
Writing – original draft: Qinglong Du.
Formal analysis: Qiyuan Wang.
Investigation: Chen Yang, Yiping Wang.
Software: Huiyang Yuan.
Supervision: Bing Zhang, Hong Ji.
Validation: Bing Zhang, Hong Ji.
Writing – review & editing: Shuai Fu, Chunlei Xue.

References

[1] Siegel RL, Giaquinto AN, Jemal A. Cancer statistics, 2024. CA Cancer J Clin. 2024;74:12–49.
[2] Scelo G, Larose TL. Epidemiology and risk factors for kidney cancer. J Clin Oncol. 2018;36:3574–81.
[3] Capitanio U, Montorsi F. Renal cancer. Lancet. 2016;387:894–906.
[4] Barata PC, Rini BI. Treatment of renal cell carcinoma: current status and future directions. CA Cancer J Clin. 2017;67:507–24.
[5] Kietrys AM, Kool ET. A new methyl mark on messengers. Nature. 2016;530:423–4.
[6] Chen Y, Hong T, Wang S, Mo J, Tian T, Zhou X. Epigenetic modification of nucleic acids: from basic studies to medical applications. Chem Soc Rev. 2017;46:2844–72.
[7] Klemm SL, Shipony Z, Greenleaf WJ. Chromatin accessibility and the regulatory epigenome. Nat Rev Genet. 2019;20:207–20.
[8] Greenberg MVC, Bourc'his D. The diverse roles of DNA methylation in mammalian development and disease. Nat Rev Mol Cell Biol. 2019;20:590–607.
[9] Robertson KD. DNA methylation and chromatin - unraveling the tangled web. Oncogene. 2002;21:5361–79.
[10] Roundtree IA, Evans ME, Pan T, He C. Dynamic RNA modifications in gene expression regulation. Cell. 2017;169:1187–200.
[11] Liu J, Dou X, Chen C, et al. N6-methyladenosine of chromosome-associated regulatory RNA regulates chromatin state and transcription. Science. 2020;367:580–6.
[12] Bannister AJ, Kouzarides T. Regulation of chromatin by histone modifications. Cell Res. 2011;21:381–95.
[13] Huang H, Weng H, Zhou K, et al. Histone H3 trimethylation at lysine 36 guides m6A RNA modification co-transcriptionally. Nature. 2019;567:414–9.
[14] Li Y, Xia L, Tan K, et al. N6-methyladenosine co-transcriptionally directs the demethylation of histone H3K9me2. Nat Genet. 2020;52:870–7.
[15] Foster BM, Stolz P, Mulholland CB, et al. Critical role of the UBL domain in stimulating the E3 ubiquitin ligase activity of UHRF1 toward chromatin. Mol Cell. 2018;72:739–52.e9.
[16] Curran MA, Montalvo W, Yagita H, Allison JP. PD-1 and CTLA-4 combination blockade expands infiltrating T cells and reduces regulatory T and myeloid cells within B16 melanoma tumors. Proc Natl Acad Sci USA. 2010;107:4275–80.
[17] Zhang X, Shi M, Chen T, Zhang B. Characterization of the immune cell infiltration landscape in head and neck squamous cell carcinoma to aid immunotherapy. Mol Ther Nucleic Acids. 2020;22:298–309.
[18] Xu Q, Chen S, Hu Y, Huang W. Landscape of immune microenvironment under immune cell infiltration pattern in breast cancer. Front Immunol. 2021;12:711433.

[19] Chen Y, Zhou C, Sun Y, He X, Xue D. m(6)A RNA modification modulates gene expression and cancer-related pathways in clear cell renal cell carcinoma. Epigenomics. 2020;12:87–99.
[20] Yao X, Tan J, Lim KJ, et al. VHL deficiency drives enhancer activation of oncogenes in clear cell renal cell carcinoma. Cancer Discov. 2017;7:1284–305.
[21] Mcdermott DF, Huseni MA, Atkins MB, et al. Clinical activity and molecular correlates of response to atezolizumab alone or in combination with bevacizumab versus sunitinib in renal cell carcinoma. Nat Med. 2018;24:749–57.
[22] Powles T, Atkins MB, Escudier B, et al. Efficacy and safety of atezolizumab plus bevacizumab following disease progression on atezolizumab or sunitinib monotherapy in patients with metastatic renal cell carcinoma in IMmotion150: a randomized phase 2 clinical trial. Eur Urol. 2021;79:665–73.
[23] Motzer RJ, Powles T, Atkins MB, et al. Final overall survival and molecular analysis in IMmotion151, a phase 3 trial comparing atezolizumab plus bevacizumab vs sunitinib in patients with previously untreated metastatic renal cell carcinoma. JAMA Oncol. 2022;8:275–80.
[24] Rini BI, Powles T, Atkins MB, et al.; IMmotion151 Study Group. Atezolizumab plus bevacizumab versus sunitinib in patients with previously untreated metastatic renal cell carcinoma (IMmotion151): a multicentre, open-label, phase 3, randomised controlled trial. Lancet. 2019;393:2404–15.
[25] Zhang Y, Liu T, Meyer CA, et al. Model-based Analysis of ChIP-Seq (MACS). Genome Biol. 2008;9:R137.
[26] Meng J, Lu Z, Liu H, et al. A protocol for RNA methylation differential analysis with MeRIP-Seq data and exomePeak R/Bioconductor package. Methods. 2014;69:274–81.
[27] Michalak EM, Burr ML, Bannister AJ, Dawson MA. The roles of DNA, RNA and histone methylation in ageing and cancer. Nat Rev Mol Cell Biol. 2019;20:573–89.
[28] Shi H, Wei J, He C. Where, when, and how: context-dependent functions of RNA methylation writers, readers, and erasers. Mol Cell. 2019;74:640–50.
[29] Knijnenburg TA, Wang L, Zimmermann MT, et al.; Cancer Genome Atlas Research Network. Genomic and molecular landscape of DNA damage repair deficiency across the cancer genome atlas. Cell Rep. 2018;23:239–54.e6.
[30] Wilkerson MD, Hayes DN. ConsensusClusterPlus: a class discovery tool with confidence assessments and item tracking. Bioinformatics. 2010;26:1572–3.
[31] Yoshihara K, Shahmoradgoli M, Martínez E, et al. Inferring tumor purity and stromal and immune cell admixture from expression data. Nat Commun. 2013;4:2612.
[32] Zaccara S, Ries RJ, Jaffrey SR. Reading, writing and erasing mRNA methylation. Nat Rev Mol Cell Biol. 2019;20:608–24.
[33] Zhao Y, Garcia BA. Comprehensive catalog of currently documented histone modifications. Cold Spring Harbor Perspect Biol. 2015;7:a025064.
[34] Liu Y, Liang G, Xu H, et al. Tumors exploit FTO-mediated regulation of glycolytic metabolism to evade immune surveillance. Cell Metab. 2021;33:1221–33.e11.
[35] Kortlever RM, Sodir NM, Wilson CH, et al. Myc cooperates with Ras by programming inflammation and immune suppression. Cell. 2017;171:1301–15.e14.
[36] Tamma R, Rutigliano M, Lucarelli G, et al. Microvascular density, macrophages, and mast cells in human clear cell renal carcinoma with and without bevacizumab treatment. Urol Oncol. 2019;37:355.e11–9.
[37] Netti GS, Lucarelli G, Spadaccino F, et al. PTX3 modulates the immunoflogosis in tumor microenvironment and is a prognostic factor for patients with clear cell renal cell carcinoma. Aging (Albany NY). 2020;12:7585–602.
[38] Lucarelli G, Rutigliano M, Ferro M, et al. Activation of the kynurenine pathway predicts poor outcome in patients with clear cell renal cell carcinoma. Urol Oncol. 2017;35:461.e15–27.
[39] Lucarelli G, Netti GS, Rutigliano M, et al. MUC1 expression affects the immunoflogosis in renal cell carcinoma microenvironment through complement system activation and immune infiltrate modulation. Int J Mol Sci. 2023;24:4814.
[40] Lasorsa F, Rutigliano M, Milella M, et al. Cellular and molecular players in the tumor microenvironment of renal cell carcinoma. J Clin Med. 2023;12:3888.
[41] Bianchi C, Meregalli C, Bombelli S, et al. The glucose and lipid metabolism reprogramming is grade-dependent in clear cell renal cell carcinoma primary cultures and is targetable to modulate cell viability and proliferation. Oncotarget. 2017;8:113502–15.
[42] Lasorsa F, Rutigliano M, Milella M, et al. Cancer stem cells in renal cell carcinoma: origins and biomarkers. Int J Mol Sci. 2023;24:16515.
[43] De Marco S, Torsello B, Minutiello E, et al. The cross-talk between Abl2 tyrosine kinase and TGFbeta1 signalling modulates the invasion of clear cell renal cell carcinoma cells. FEBS Lett. 2023;597:1098–113.